JACS
JOURNAL OF THE AMERICAN CHEMICAL SOCIETY

Communication

pubs.acs.org/JACS

Design, Synthesis, and Characterization of Mesogenic Amine-Capped Nematic Gold Nanoparticles with Surface-Enhanced Plasmonic Resonances

Chih H. Yu, Christopher P. J. Schubert, Chris Welch, Bai J. Tang, M.-Gabriela Tamba, and Georg H. Mehl*

Department of Chemistry, University of Hull, Cottingham Road, Hull HU6 7RX, United Kingdom

Supporting Information

ABSTRACT: The use of the liquid-crystalline state to control the assembly of large (>5 nm) gold nanoparticles (NPs) is of considerable interest because of the promise of novel metamaterial properties of such systems. Here we report on a new approach for the preparation of large nematic gold NPs using a bifunctional capping agent that enables control over the particle size and serves as a linkage for subsequent functionalization with mesogenic groups. Properties of the NPs were characterized by HRTEM, NMR, DSC, TGA, UV/vis, OPM, and XRD studies. The results confirmed the formation of a stable nematic mesophase above 37.5 °C for NPs in the 6−11 nm size range.

Gold nanoparticles (NPs) functionalized with mesogenic groups[1−5] have recently attracted considerable attention as potential candidates for metamaterials with tuned optic-electric behavior, enhanced plasma-splitting properties, and electrically controlled light-scattering properties.[6−10] The physical and optical properties of the NPs are strongly affected by the size and shape of the particles and by the chemical structure of the attached organic ligands. Moreover, the design of the organic corona affects the self-assembly, and thus, chemical control of the composition of the particles is critical. This is particularly important because small gold particles in the 1−2 nm size range are known to exhibit quantum size effects[11] and only larger gold particles (>6 nm) show strong surface plasmatic properties critical for metamaterial behavior.[12,13] For relatively small particles in the 1.4−3 nm range that are capped with a corona of thiol-bonded hydrocarbon groups terminated with mesogenic groups, formation of a liquid crystal (LC) phase has been reported, and 2D and 3D self-assembly of the Au NPs has been detected.[1,7,8c] In most cases, mesomorphic behavior has been introduced in polymer-like exchange reactions with molecules promoting mesomorphic phase behavior after the synthesis of the NPs, following the classical Brust−Schiffrin method or using Murray's exchange ligands.[3,4,8,14−16]

However, with increasing size of the particles and the concomitant increase in the size of the ensuing organic corona, it was found that the control of mesomorphic properties becomes more difficult and that the viscosities of the materials, which determine to some extent their technological potential in thin films, increase significantly. Moreover, because of the small size of the particles (typically less than 3 nm), they may exhibit various morphological structures other than the typically most stable face-centered-cubic (fcc) structure that would be expected under thermodynamic control.[17]

Thus, it is an important challenge to prepare Au NPs with sizes larger than 6 nm, where plasmonic effects play a strong role, and to design an organic corona that promotes self-assembly and allows for the modulation of the viscosities of the target materials.

To address these issues, a novel two-step approach was pursued (Figure 1). In the first step, NPs capped with organic chains bearing reactive end groups were prepared. In the second step, reactions of these end groups to introduce groups that lower the viscosity and induce mesomorphic behavior were carried out. As a capping agent, amine functionalities were used, as it was found that the classical approach for NPs (<6 nm) using thiol groups as capping agents did not yield acceptable results. In initial experiments, the thiol groups were found to

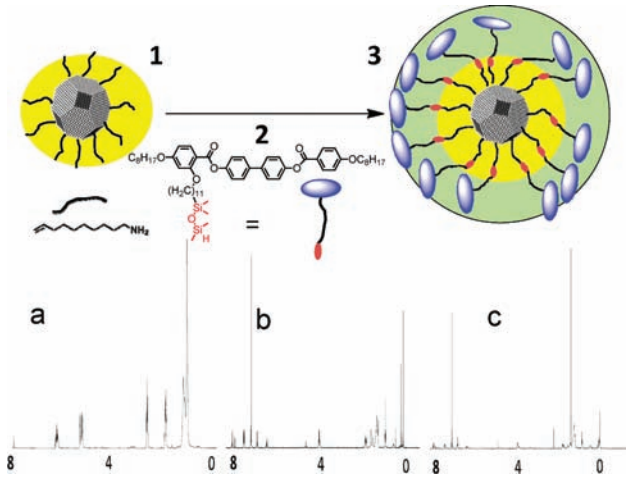

Figure 1. (top) Structures of dec-9-enylamine-functionalized organic-coated Au NPs (**1**), the mesogen (**2**), and mesogen-coated Au NPs (**3**). (bottom) NMR spectra of (a) dec-9-enylamine-functionalized Au NPs, (b) the mesogen, and (c) nematic Au NPs.

Received: February 2, 2012
Published: March 5, 2012

 © 2012 American Chemical Society dx.doi.org/10.1021/ja300492d | J. Am. Chem. Soc. 2012, 134, 5076−5079

interfere with reactions of the organic corona involving transition-metal catalysts. Since the successful synthesis of larger particles using primary amines as ligands has been reported previously, this route was pursued.[18,19] To modulate the melting behavior, a tetramethyldisiloxane unit, a group known to lower thermal transition temperatures, was introduced into the hydrocarbon chain. Laterally connected mesogens were used to induce LC behavior in the Au NPs.[20]

For the synthesis of larger NPs (>6 nm), a water/oil microemulsion technique was developed. This method was adapted from earlier work on the synthesis of iron oxide particles.[21,22] To obtain Au NPs in the 6−11 nm size range, it was found that the optimal molar ratio of water to tetraoctylammonium bromide (TOAB, used as a surfactant) was 18.4 [for details, see the Supporting Information (SI)].[25] Dec-9-enylamine was prepared and used as a digestive-ripening capping agent bearing a terminal alkene group for post-NP-synthesis functionalization.[23]

The ^{1}H NMR spectrum of the NPs (Figure 1a) confirmed that all of the impurities (e.g., TOAB, $NaBH_4$, and dodecylamine) were removed by washing using ethanol or acetone. In addition, the alkene group in the functionalized Au NPs can be clearly observed from the ^{1}H NMR signals at δ 5.70−5.80 (m, 1H, CH) and 4.85−5.00 (m, 2H, CH_2). Moreover, the ^{1}H NMR spectrum of the NPs (Figure 1a) confirmed the chemical composition of the material and the attachment of the amine group to the gold surface, as evidenced by the absence of the signal for the protons adjacent to the amine group. The accuracy of these measurements was tested in additional experiments by adding dec-9-enylamine (5% w/w) to the purified capped NPs, and here a signal for the protons in the methylene group adjacent to the amine functionality could be detected. This shows that in the purified NPs no free amine groups were present, and this result was confirmed by thin-layer chromatography (TLC) and gel-permeation chromatography (GPC) experiments (see the SI).

As a surface functionalization reaction method, the hydrosilylation of terminal olefin groups mediated by Karstedt's catalyst was selected. In successful tests with pentamethyldisiloxane, complete functionalization of the organic surface was observed, as evidenced by the disappearance of the signals for the terminal olefin groups at δ 5.7−5.8 (−CH) and 4.85−5.0 ($-CH_2$) and the appearance of signals at δ 0.3 ($-CH_2$) and 0.15 from the five methyl groups of the pentamethyldisiloxane group. Subsequently the organic mesogenic group **2** bearing a reactive silane group (Figure 1) was selected as a suitable LC moiety. This particular group was selected on the basis of its structural similarity with related mesomorphic Au NP systems previously reported.[8] The use of a siloxane functionality permitted attachment to the organic surface of the NPs while decreasing the viscosity and melting point of the system.[20]

The rodlike mesogen **2** contains four aromatic rings with eight methylene groups as flexible chains and melts at 97.7 °C into a nematic phase before clearing to an isotropic liquid at 115.7 °C. This nematic-to-isotropic transition is associated with an enthalpy of 0.59 J g^{-1}, a somewhat low value for a low-molar-mass calamitic nematic system that is attributed to the presence of the long lateral chain bearing a siloxane group. Following the hydrosilylation reaction using Karstedt's catalyst in dry toluene at room temperature, removal of the excess LC group monomer was carried out, initially by intensive washing and subsequently by size-exclusion chromatography (SEC) with Biobeads SX-1 as the stationary phase and tetrahydrofuran as the solvent. The chemical structure of the organic corona surrounding the NP **3** was confirmed by ^{1}H NMR spectroscopy (Figure 1c). The signals relating to the alkene and silane groups were no longer present in the spectrum [peaks at δ 5.7−5.8 (−CH), δ 4.85−5.0 ($-CH_2$), and δ 4.65−4.68 (−SiH)]. The attachment of the amine function to the gold surface was evidenced by the absence of the signals of the methylene group connected to the amine function at δ 2.65−2.85 ($-CH_2-NH_2$). TLC and GPC experiments confirmed the high purity of the material.

High-resolution transmission electron microscopy (HRTEM) (Figure 2a,c; also see the SI) confirmed that the

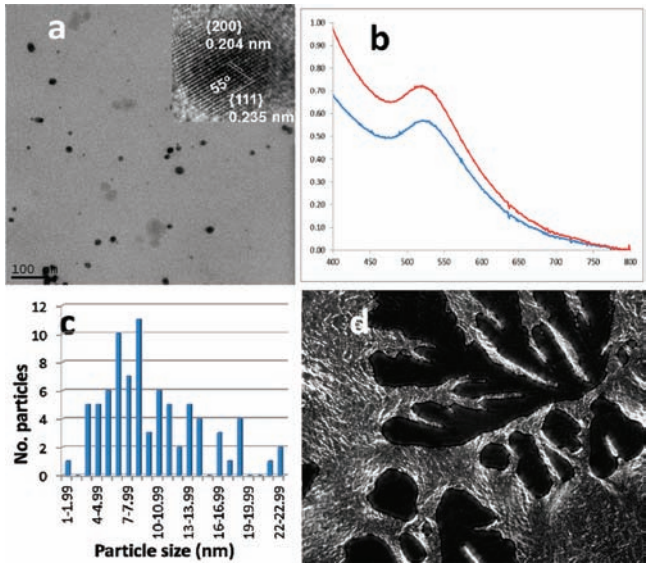

Figure 2. (a) TEM image of nematic Au NPs. (b) UV/vis spectra of nematic Au NPs with SPRs at ∼520 nm before (blue) and after (red) size exclusion. (c) Histogram depicting the size distribution of the particles. (d) OPM texture of nematic Au NPs at 60 °C (×100).

size of the Au NPs ranged from 6 to 18 nm (average size 9.98 ± 2.2 nm) (see the SI). As shown in the histogram of the size distributions of the NPs (Figure 2c), the majority of the NPs have sizes of 6−11 nm, although larger particles are found as well, shifting the average size to a value close to 10 nm. The lattice-fringe spacings of the Au NPs were confirmed as d_{hkl} = 0.235 nm {111} and 0.204 nm {200} with 55° crossover (Figure 2a inset). The image shows the {111} planes of an fcc structure of the Au NP, and this is the most stable facet. It is likely that the geometry exhibits truncated icosahedral or decahedral NPs.[8,24] The size and structure of the material before coating with mesogen was also confirmed by powder X-ray diffraction (XRD).[25]

The Au NPs show intensive surface plasmon resonances (SPRs), as confirmed by UV/vis spectrometry, which showed a maximum at ∼520 nm with only a single peak, a feature typical for spherical Au NPs (Figure 2b).[27] The spectra in Figure 2b show the UV/vis adsorption before (blue line) and after (red line) purification by SEC. The two spectra exhibit similar positions of the SPR, indicating, according to Mie theory,[26] that the purification process removed the low-molar-mass impurities without fundamentally altering the structure of the NPs.

The LC properties of **3** were investigated by optical polarization microscopy (OPM) and differential scanning calorimetry (DSC), and the results are shown in Table 1.

dx.doi.org/10.1021/ja300492d | J. Am. Chem. Soc. 2012, 134, 5076−5079

Table 1. Transition Temperatures (T_{trans}) and Enthalpies (ΔH_{trans}) Determined by DSC[a]

compound	transition	T_{trans}/°C	transition	T_{trans}/°C (ΔH_{trans}/J g^{-1})
2	Cr → N	97.7	N → Iso	115.7 (0.59)
3	Cr → N	37.5	N → Iso	94.5 (2.76)

[a]The scan rate was 10 °C min^{-1} in the heating cycle. Abbreviations: Cr, crystalline phase; N, nematic LC phase; Iso, isotropic phase.

DSC experiments revealed a melting point of 37.5 °C in freshly prepared samples. The material cleared from an LC phase to an isotropic phase at 94.5 °C, a transition associated with an enthalpy change of 2.76 J g^{-1}. Relative to the monomeric material (mesogen **2** in Figure 1), the isotropization temperature was reduced by 21.2 °C; however, as the melting point was reduced by 60.3 °C, the LC range increased by ∼39.1 °C. A decrease in the transition temperature has been observed previously in Au NPs functionalized with laterally connected LC groups as well as in other LC NPs and can be attributed to a destabilization of the LC phase due to the presence of the central nondeformable NP core, which reduces the orientational mobility of the mesogens, differentiating the NPs from LC dendrimers.[7a,8,10] The lowering of the melting point is attributed to the increased spacer length relative to earlier results but is mainly due to the inclusion of the disiloxane group in the middle of the spacer unit separating the NP and the mesogens. OPM studies confirmed the nematic structure of the mesophase; a typical OPM micrograph showing the formation of a coarse-grained gray schlieren-type texture is presented in Figure 2d. In comparison with other reported materials, compound **3** is characterized by the rapid formation of a defect texture, indicative of a relatively low viscosity, and shearing of the sample by moving the microscopy coverslip is easily possible. Preliminary XRD experiments on nonoriented samples in the nematic phase were carried out. It should be noted that aligning the samples by shearing or the use of capillary force was not possible. Weak reflections at $2\Theta = 3.32°$, 17.62° (broad), and 18.89° (broad), equivalent to d = 2.66, 0.507, and 0.470 nm, respectively, were detected (see the SI). The wide-angle reflections can be associated with the liquidlike ordering of the hydrocarbon and siloxane chains and the mesogenic groups. The reflection at d = 2.66 nm can be associated with the longitudinal dimension of the aromatic core of the mesogens and is close to the d value of 2.80 nm detected for **2** (see the SI). Though an increase in the diffracted scattering intensities at smaller angles that could not be attributed to background scattering was detected, no indication of the formation of long-range positional ordering of the NPs was found. This increase of the scattering intensity is likely to be associated with local short-range ordering of the particles assumed to be distributed in the nematic organic matrix.[28]

In summary, we have designed and prepared mesogenic-group-coated Au NPs in which the organic ligands are linked to the NPs via amine groups. A novel two-step approach was used. First, Au NPs were prepared by a digestive ripening method, using a microemulsion of appropriate size for plasmonic properties, and then capped with end-group-functionalized ligands. The mesomorphic group was introduced in the second step by a reaction of the organic surface. The use of a long spacer that includes a siloxane group helped to lower the viscosity. The resulting materials are thermally and chemically stable and show nematic phase behavior close to room temperature.

■ ASSOCIATED CONTENT

Supporting Information

Synthesis procedures for **1**−**3** and TEM, DSC, GPC, NMR, and XRD characterizations. This material is available free of charge via the Internet at http://pubs.acs.org.

■ AUTHOR INFORMATION

Corresponding Author

g.h.mehl@hull.ac.uk

Notes

The authors declare no competing financial interest.

■ ACKNOWLEDGMENTS

This research was supported by the EU under Grant 228455.

■ REFERENCES

(1) Wojcik, M.; Lewandowski, W.; Matraszek, J.; Mieczkowski, J.; Borysiuk, J.; Pociecha, D.; Gorecka, E. *Angew. Chem., Int. Ed.* **2009**, *48*, 5167−5169.
(2) Gupta, V. K.; Abbott, N. L. *Langmuir* **1996**, *12*, 2587−2593.
(3) Kanayama, N.; Tsutsumi, O.; Kanazawa, A.; Ikeda, T. *Chem. Commun.* **2001**, 2640−2641.
(4) In, I.; Jun, Y. W.; Kim, Y. J.; Kim, S. Y. *Chem. Commun.* **2005**, 800−801.
(5) Gupta, V. K.; Miller, W. J.; Pike, C. L.; Abbott, N. L. *Chem. Mater.* **1996**, *8*, 1366−1369.
(6) Rockstuhl, C.; Lederer, F.; Etrich, C.; Pertsch, T.; Scharf, T. *Phys. Rev. Lett.* **2007**, *99*, No. 017401.
(7) (a) Donnio, B.; García-Vázquez, P.; Gallani, J.-L.; Guillon, D.; Terazzi, E. *Adv. Mater.* **2007**, *19*, 3534−3539. (b) Draper, M.; Saez, I. M.; Cowling, S. J.; Gai, P.; Heinrich, B.; Donnio, B.; Guillon, D.; Goodby, J. W. *Adv. Funct. Mater.* **2011**, *21*, 1260−1278.
(8) (a) Cseh, L.; Mehl, G. H. *J. Am. Chem. Soc.* **2006**, *128*, 13376−13377. (b) Cseh, L.; Mehl, G. H. *J. Mater. Chem.* **2007**, *17*, 311−315. (c) Zeng, X. B.; Liu, F.; Fowler, A. G.; Ungar, G.; Cseh, L.; Mehl, G. H.; Macdonald, J. E. *Adv. Mater.* **2009**, *21*, 1746−1750.
(9) (a) Qi, H.; Hegmann, T. *J. Mater. Chem.* **2006**, *16*, 4197−4205. (b) Marx, V. M.; Girgis, H.; Heiney, P. A.; Hegmann, T. *J. Mater. Chem.* **2008**, *18*, 2983−2994.
(10) Frein, S.; Boudon, J.; Vonlanthen, M.; Scharf, T.; Barbera, J.; Suss-Fink, G.; Burgi, T.; Deschenaux, R. *Helv. Chim. Acta* **2008**, *91*, 2321−2337.
(11) Link, S.; El-Sayed, M. A. *Int. Rev. Phys. Chem.* **2000**, *19*, 409−453.
(12) Daniel, M. C.; Astruc, D. *Chem. Rev.* **2004**, *104*, 293−346.
(13) Peng, S.; McMahon, J. M.; Schatz, G. C.; Gray, S. K.; Sun, Y. *Proc. Natl. Acad. Sci. U.S.A.* **2010**, *107*, 14530−14534.
(14) Brust, M.; Walker, M.; Bethell, D.; Schiffrin, D. J.; Whyman, R. *J. Chem. Soc., Chem. Commun.* **1994**, 801−802.
(15) Kumar, S.; Pal, S. K.; Kumar, P. S.; Lakshminarayanan, V. *Soft Matter* **2007**, *3*, 896−900.
(16) Hostetler, M. J.; Green, S. J.; Stokes, J. J.; Murray, R. W. *J. Am. Chem. Soc.* **1996**, *118*, 4212−4213.
(17) Barnard, A. S.; Lin, X. M.; Curtiss, L. A. *J. Phys. Chem. B* **2005**, *109*, 24465−24472.
(18) Prasad, B. L. V.; Stoeva, S. I.; Sorensen, C. M.; Klabunde, K. J. *Chem. Mater.* **2003**, *15*, 935−942.
(19) Yang, J.; Ying, J. Y. *Nat. Mater.* **2009**, *8*, 683−689.
(20) Filip, D.; Cruz, C.; Sebastiao, P. J.; Cardoso, M.; Ribeiro, A. C.; Vilfan, M.; Meyer, T.; Kouwer, P. H. J.; Mehl, G. H. *Phys. Rev. E* **2010**, *81*, No. 011702.
(21) Tsang, S. C.; Yu, C. H.; Gao, X.; Tam, K. *J. Phys. Chem. B* **2006**, *110*, 16914−16922.
(22) Yu, C. H.; Al-Saadi, A.; Shih, S.-J.; Qiu, L.; Tam, K. Y.; Tsang, S. C. *J. Phys. Chem. C* **2009**, *113*, 537−534.
(23) Kaur, N.; Delcros, J. G.; Martin, N.; Phanstiel, O. *J. Med. Chem.* **2005**, *48*, 3832−3839.

(24) Ascencio, J. A.; Perez, M.; Jose-Yacaman, M. *Surf. Sci.* **2000**, *447*, 73−80.
(25) Powder XRD data and the Debye−Scherrer equation were used to estimatate the size of the NPs to be ∼6.32 nm, a value in line with the TEM data, taking into account the polydispersity of the NPs.
(26) Daniel, M. C.; Ruiz, J.; Nlate, S.; Blais, J. C.; Astruc, D. *J. Am. Chem. Soc.* **2003**, *125*, 2617−2628.
(27) Amendola, V.; Meneghetti, M. *J. Phys. Chem. C* **2009**, *113*, 4277−4285.
(28) No distinct reflections were detected up to $2\Theta = 6.4°$, the lower angular limit for the employed equipment.